Eur Respir J 2002; 20: 1545–1558
DOI: 10.1183/09031936.02.00062102
Printed in UK – all rights reserved

European Respiratory Journal
ISSN 0903-1936

SERIES "CONTRIBUTIONS FROM THE EUROPEAN RESPIRATORY MONOGRAPH"
Edited by M. Decramer and A. Rossi
Number 12 in this Series

Physiology and pathophysiology of pleural fluid turnover

L. Zocchi

Physiology and pathophysiology of pleural fluid turnover. L. Zocchi. ©ERS Journals Ltd 2002.

ABSTRACT: Tight control of the volume and composition of the pleural liquid is necessary to ensure an efficient mechanical coupling between lung and chest wall. Liquid enters the pleural space through the parietal pleura down a net filtering pressure gradient. Liquid removal is provided by an absorptive pressure gradient through the visceral pleura, by lymphatic drainage through the stomas of the parietal pleura, and by cellular mechanisms. Indeed, contrary to what was believed in the past, pleural mesothelial cells are metabolically active, and possess the cellular features for active transport of solutes, including vesicular transport of protein. Furthermore, the mesothelium was shown, on the basis of recent experimental evidence, both *in vivo* and *in vitro*, to be a less permeable barrier than previously believed, being provided with permeability characteristics similar to those of the microvascular endothelium. Direct assessment of the relative contribution of the different mechanisms of pleural fluid removal is difficult, due to the difficulty in measuring the relevant parameters in the appropriate areas, and to the fragility of the mesothelium. The role of the visceral pleura in pleural fluid removal under physiological conditions is supported by a number of findings and considerations.

Further evidence indicates that direct lymphatic drainage through the stomas of the parietal pleura is crucial in removing particles and cells, and important in removing protein from the pleural space, but should not be the main effector of fluid removal. Its importance, however, increases markedly in the presence of increased intrapleural liquid loads. Removal of protein and liquid by transcytosis, although likely on the basis of morphological findings and suggested by recent indirect experimental evidence, still needs to be directly proven to occur in the pleura. When pleural liquid volume increases, an imbalance occurs in the forces involved in turnover, which favours fluid removal. In case of a primary abnormality of one ore more of the mechanisms of pleural liquid turnover, a pleural effusion ensues. The factors responsible for pleural effusion may be subdivided into three main categories: those changing transpleural pressure balance, those impairing lymphatic drainage, and those producing increases in mesothelial and capillary endothelial permeability. Except in the first case, pleural fluid protein concentration increases above normal: this feature underlies the classification of pleural effusions into transudative and exudative.

Eur Respir J 2002; 20: 1545–1558.

Correspondence: L. Zocchi
Istituto di Fisiologia Umana I
via Mangiagalli 32
20133 Milan
Italy

Keywords: Exudate
lymphatics
mesothelium
pleural effusion
Starling forces
transudate

Received: July 10 2002
Accepted after revision: August 1 2002

The thin layer of liquid present between the pleural surfaces has the important function of providing the mechanical coupling between the chest wall and lung, which ensures instantaneous transmission of perpendicular forces between the two structures, and allows their sliding in response to shearing forces [1, 2]. It also provides lubrication of the reciprocal motions of the two structures during breathing. Two views, in part compatible, exist on the nature of the mechanisms providing the mechanical coupling between the lung and chest wall. They have been extensively described and reviewed elsewhere [1–11].

Previous articles in this series: No. 1: Baldacci S, Omenaas E, Oryszczyn MP. Allergy markers in respiratory epidemiology. *Eur Respir J* 2001; 17: 773–790. **No. 2:** Antó JM, Vermeire P, Vestbo J, Sunyer J. Epidemiology of chronic obstructive pulmonary disease. *Eur Respir J* 2001; 17: 982–994. **No. 3:** Cuvelier A, Muir J-F. Noninvasive ventilation and obstructive lung diseases. *Eur Respir J* 2001; 17: 1271–1281. **No. 4:** Wysocki M, Antonelli M. Noninvasive mechanical ventilation in acute hypoxaemic respiratory failure. *Eur Respir J* 2001; 18: 209–220. **No. 5:** Østerlind K. Chemotherapy in small cell lung cancer. *Eur Respir J* 2001; 18: 1026–1043. **No. 6:** Jaakkola MS. Environmental tobacco smoke and health in the elderly. *Eur Respir J* 2002; 19: 172–181. **No. 7:** Hollings N, Shaw P. Diagnostic imaging of lung cancer. *Eur Respir J* 2002; 19: 722–742. **No. 8:** Künzli N. The public health relevance of air pollution abatement. *Eur Respir J* 2002; 20: 198–209. **No. 9:** D′Amato G, Liccardi G, D′Amato M, Cazzola M. Outdoor air pollution, climatic changes and allergic bronchial asthma. *Eur Respir J* 2002; 20: 763–776. **No. 10:** Pelosi P, Brazzi L, Gattinoni L. Prone position in acute respiratory distress syndrome. *Eur Respir J* 2002; 20: 1017–1028. **No. 11:** Sartori C, Matthay MA. Alveolar epithelial fluid transport in acute lung injury: new insights. *Eur Respir J* 2002; 20: 1299–1313.

For the coupling to be effective, the volume of pleural liquid required for lubrication must be kept down to a minimum [1, 2], and the colloidosmotic pressure must be low in order to keep this volume small. On the other hand, liquid tends to be drawn into the space, along with small solutes and, to a lesser extent, protein, because the recoils of lung and chest wall act as opposing forces over most of the range of respiratory volumes. The pressure acting on the pleural surface (P_{pl}) at midlung height averages $\sim$-6 cmH_2O during a tidal breath, becomes more negative with deeper breaths, and is more negative at the top of the space than at the bottom, decreasing by $\sim$0.2 $cmH_2O \cdot cm^{-1}$ height in man, and 0.5–0.7 $cmH_2O \cdot cm^{-1}$ in dogs and rabbits (reviewed in [1–3]). The control of volume and composition of the pleural liquid is affected by a number of mechanisms removing from the pleural space the liquid filtered from the parietal pleura, small solutes and protein. They include the Starling forces through the mesothelium and the adjacent connective tissue capillaries, the lymphatic drainage through the parietal pleura stomata, and the activity of mesothelial cells. This review will discuss the present knowledge concerning these mechanisms and their relative contributions to pleural fluid turnover. While the first two mechanisms, described long ago, have received great attention and evoked lively debates, cellular mechanisms involved in pleural fluid turnover have until recently been neglected. Relevance will be given to the role of mesothelial cells in transpleural transport, namely to their solute-coupled liquid absorption [12], and to recent findings on vesicular transport of protein.

Morphological basis of transpleural exchange

The total surface area of the visceral pleura (both cavities) is $\sim$220 cm^2 in 2 kg rabbits, and $\sim$1,000 cm^2 in 9 kg dogs [13]; that of the parietal pleura, computed from that facing the lungs [13] plus that of the costophrenic sinuses, is approximately the same. Pleural surface area roughly increases in proportion to body $mass^{2/3}$ (a measure of surface area: body weight to the 2/3 power); it should be $\sim$4,000 cm^2 in a 70 kg man. The pleurae comprise a layer of mesothelial cells and the underlying connective tissue [14–19]. The cytological, cytochemical and structural features of the mesothelial cells are common to all serosae in a variety of animal species (man, sheep, pig, dog, rabbit) [19–22], supporting the view of the mesothelium as an entity [22]. Contrary to the past, when mesothelial cells were thought to merely provide a passive envelope to serosal cavities, they are now recognised as active cells, involved in many structural and metabolic functions [15, 19, 23–26]. They are provided with abundant organelles, extensive cytoskeleton, ribonucleic acid, glycogen stores, and enzymatic activities [15, 19, 22, 26]; they synthesise macromolecules of the underlying connective tissue, and biologically active molecules [19, 23]; they are reactive cells, responding to inflammatory stimuli with increases in the above activities, expression of more enzymes, release of cytokines, growth factors and chemotactic peptides [15, 19, 23, 24].

A key function of the mesothelium, long overlooked, is its active role in transerosal transport. Pleural mesothelial cells possess all the features required for active transport [25], and hints for such transport through the visceral pleura have been found since 1977 [26]. Proof of the expression of active transcellular transporters in peritoneal mesothelium [27], and indirect evidence for a solute-coupled liquid transport across the pleura [8, 28–35] have now been provided. The apical microvilli of mesothelial cells [14–16, 18–22, 36] increase the surface area available for exchange, and may act in association with vesicles (see below) in transcellular transport [19, 37]. Their density (ranging from 2–6 μm^{-2} [36] to 30 μm^{-2} [16]) displays regional variations, being greater in the caudal regions, and in the visceral than in the parietal pleura [18]. Their number increases after intraperitoneal injection of albumin [37], and when the mesothelial cell is activated [19]. They also contribute to reducing friction between the visceral and parietal mesothelia, through the glycoproteins rich in hyaluronic acid (secreted by mesothelial cells) they entrap [36]. Phospholipids are adsorbed to the apical surface of mesothelial cells [38, 39]: they provide boundary lubrication (appropriate for the slowly moving pleurae) at points where no liquid is interposed between cells, and reduce mesothelial permeability [40–43], as they do in epithelia [44]. Mesothelial cells are joined in the apical part of the intercellular space by junctional complexes [15, 16, 18, 19–22], comprising 1–5 stranded tight junctions 8–9 nm wide, similar to those of venular endothelium [19]. Accordingly, in line with the notion that openings in these junctions represent the diffusional pathway for small solutes [45–48], the permeability of the mesothelium to small solutes is similar to that of microvascular endothelium [40, 41, 43]. Finally, numerous free cytoplasmic vesicles, 40–60 nm in diameter, are observed in mesothelial cells [15, 16, 18–22, 25]; coated vesicles, responsible for receptor-mediated endocytosis were also found [15]. Analogous to what is known about the endothelium [48], morphologists have emphasised their role in protein transfer [15, 18, 19, 25]. Conversely, most physiologists interested in exchanges across the pleura generally neglected, or dismissed, any role of transcytosis in protein removal from the pleural space, attributing this function exclusively to lymphatic stomas (see below).

The submesothelial connective tissue contains blood vessels and lymphatics [14, 17–22, 25, 35]. Fibres (type I and III collagen, elastin) are distributed with varying density and orientation in the interstitial matrix (glycoprotein, proteoglycans and water), organised in different layers. Water and solutes flow in the free channels between fibres; the restriction to diffusion of water and solutes (including macromolecules) offered by the submesothelial connective tissue is negligible [40–43]. Connective tissue thickness determines the overall thickness of a serosa (mesothelial cells being only 2 μm thick [18]) and it varies across species, serosae, and regions of a serosa. The parietal pleura thickness increases with animal size (from $\sim$7 μm in

mice [10] to 30–40 μm in man), and is fairly constant throughout the space. Parietal pleura capillaries, supplied by systemic arteries, are ~10–15 μm from the mesothelium in sheep and rat [17, 35] and more distant in man [35]. The visceral pleura is thin (~15–35 μm) and supplied by pulmonary arteries, in some animal species (dog, cat, rabbit) [35], while it is thicker in other species (man, sheep, pig), the difference mainly concerning the caudal lobe [14]. In sheep, thickness is 15–86 μm in the caudal lobe, and 9–27 μm in middle and cranial ones [14, 17]. In the species with thick visceral pleura, most of the blood supply is from the systemic bronchial arteries [14, 35]. However, pleural capillary pressure (affecting the pressure balance implied in transmesothelial liquid flows) should be similar in thick and thin pleura, since in both cases the capillaries drain into the low pressure pulmonary veins. Capillaries are found in close proximity to the visceral mesothelium in both kinds of pleura (~4 μm in rodents and ~10 μm in man [35]; they are more distant in sheep (20–50 μm [17]).

In the parietal pleura of the caudoventral mediastinum, caudal intercostal spaces and diaphragm, the submesothelial lymphatic system directly communicates with the pleural space through openings between mesothelial cells (stomas) [19, 49–51]. The extensive network of submesothelial lymphatic lacunae drains into collecting vessels, and lymph reaches the right lymphatic trunk and the thoracic duct *via* mammary, intercostal, and mediastinal lymphatics. Stoma diameter is 1–6 μm [49], and increases with inspiratory stretch [50]; their density varies among species (1–80·mm^{-2} in rabbits [49, 50], 300–400·mm^{-2} in mice [51], 1,000–2,000·mm^{-2} in sheep [17]), and between regions of the parietal pleura. In rabbits, they are ~80 times more dense in the diaphragmatic than in the intercostal pleura [49, 50], and absent in the apical regions. Recently, stomas were also found in man [52]. Stomas are the only pathway for cells and particle egress, while protein could also exit the pleural space by solvent drag and transcytosis, possibilities rarely considered [2, 4, 53]. The controversies on the contribution of lymphatic drainage through the stomas to pleural liquid absorption [3–6, 17, 54–56] are discussed below. Stomas are not found in the visceral pleura [18, 19]; therefore, no direct communication exists between the pleural space and the rich network of submesothelial lymphatics covering the lung surface. This system collects the protein and part of the fluid that crossed the visceral pleura, reaches the peribronchovascular lymphatics, and eventually drains into the the right lymphatic duct or the thoracic duct *via* the mediastinal lymphatic system.

Pleural liquid

The total volume of liquid contained in both pleural spaces is ~1 mL (~0.45 mL·kg^{-1}) in rabbits, and ~2.4 mL (~0.25 mL·kg^{-1}) in dogs [13]. This includes the liquid that cannot be collected, because it adheres to the walls of the space (0.30) (0.52 mL in rabbits [13, 57], and 1.80 mL in dogs [13]), and the liquid that can be collected (0.13–0.20 mL·kg^{-1} in rabbits [8, 13, 57, 58], and 0.06–0.10 mL·kg^{-1} in dogs [13, 59]. In sheep, 0.08 mL·kg^{-1} can be collected [60, 61]. When related to a measure of surface area (body weight to the 2/3 power), this volume ranges 0.13–0.27 mL·kg$^{-2/3}$. The total volume of pleural liquid in humans, as recently determined by urea dilution in subjects undergoing thoracoscopy for treatment of hydiopathic hyperhydrosis, is 0.26 mL·kg^{-1} [62]. The composition of pleural liquid is essentially that of a plasma filtrate through two membranes with similar sieving properties [29, 40–43, 63, 64], the capillary endothelium and the parietal pleura mesothelium. The protein concentration in pleural liquid (C_{liq}), and its ratio to that in capillary plasma (C_c) are low, implying that the permeability to protein of the pleura must be low (see Permeability characteristics). Albumin is a greater fraction of total protein in pleural liquid than in plasma [13, 65]. C_{liq} and C_{liq}/C_c decrease with increasing animal size and with maturation. This is due to an increase in the filtration rate (caused by increased systemic capillary pressure and decreased pleural liquid pressure (P_{liq})), and in lymphatic drainage [55, 60, 65]. C_{liq} ranges ~0.9–2.5 g·dL^{-1}, and C_{liq}/C_c ~0.17–0.5 from sheep to rat [13, 57, 58, 60, 61, 65]. C_{liq} increases with ventilation, suggesting that shear stress in the liquid increases pleura permeability [5]. Na^+ concentration is lower, and HCO_3^- concentration higher in pleural liquid than in serum, in line with Donnan equilibrium [28], and pH is higher than in serum (~7.6); Cl^- concentration is lower than in serum [28, 58], and glucose concentration similar to that in serum [58]. The pleural liquid in rabbits and dogs contains 1,500–2,500 cells·mm^{-3}: mesothelial cells (9–30%), monocytes/macrophages (61–77%), lymphocytes (7–11%), and neutrophils (<2%) [13, 57, 58, 66]. Approximately 1,700 cells·mm^{-3} were recently found in human normal pleural liquid (75% macrophages, 23% lymphocytes, and 1% mesothelial cells [62]). Free mesothelial cells are generally esfoliated elements, though normal, even proliferating cells are also found; polymorphonuclear (PMN) leucocytes reach the pleural space from subpleural capillaries, lymphocytes also through lymphatic stomas, monocytes/macrophages may also develop from mesothelial cells, with which they share a common mesodermal origin [62]. Pleural liquid thickness (θ), measured by different methods [1–6], is 5–24 μm in many animal species. θ is fairly independent of height, being only 2 μm greater in dependent than in superior regions of the pleural space, and only increasing after injection of >2 mL saline into the space. As expected on geometrical grounds, a three-fold increase in lung volume nearly halves θ. At the lobar edges θ is 100–1,000 μm.

Pleural fluid turnover under physiological conditions

The volume of pleural liquid (V_{liq}) results from a balance of liquid in- and outflow, occurring by Starling forces (providing filtration through the parietal, and absorption through the visceral mesothelium) [1, 2], lymphatic drainage through the parietal pleura stomas [17, 49, 67, 68], and electrolyte-coupled

liquid absorption through the mesothelium of both sides [6, 8]. According to the classic Starling equation, transpleural liquid flows (J_v) are related to the overall pressure difference (ΔP) across the visceral, or the parietal pleura, by the equation:

$$J_v = \mathrm{LpS}\Delta P \quad (1)$$

where Lp is the hydraulic conductivity (a measure of water permeability), and S the surface area of the pleura. The product LpS corresponds to the filtration coefficient (Kf). ΔP is given by:

$$[(P_c - P_{liq}) - \sigma(\pi_{liq} - \pi_c)] \quad (2)$$

where P_c is the hydraulic pressure in subpleural capillaries, π_{liq} and π_c the colloidosmotic pressure in pleural liquid and subpleural capillaries, respectively, and σ the reflection coefficient to protein of the pleural mesothelium. Solute fluxes through the pleurae (J_s), in keeping with those through capillary endothelium, are viewed as resulting from both convection, solutes being dragged by J_v, and diffusion:

$$J_s = J_v(1 - \sigma f)C + P_d S \Delta C \quad (3)$$

where σf is the solvent drag reflection coefficient for the solute, ΔC the transmesothelial solute concentration gradient, and P_d the diffusional permeability of the pleura to the solute. Vesicular transport provides an additional contribution in the endothelium [48]. Permeability to protein is relevant in determining transpleural colloidosmotic pressure.

The transfer of liquid and solutes across cell layers is often described as occurring through aqueous channels ("pores"). The pore theory of permeability, formulated for microvascular endothelium by PAPPENHEIMER *et al.* [69], and recently reviewed [48], provides a reference model in this regard. In the model, small solutes (up to the size of inulin) diffuse through "small pores" with a radius (r) of 4–5 nm, represented by clefts in the intercellular junctions. Macromolecules, too large to diffuse through these "pores", use a population of "large pores" (r=20–30 nm), less numerous than small "pores" (1:1,000 to 1:4,000), which could either be real openings or be provided by transient fusion of vesicles through the cell [48, 70]. Vesicular transport (transcytosis) contributes to the transfer of all molecules, and is essential for that of large macromolecules. In addition to these pathways, water also flows through water-exclusive channels (aquaporins) of the cell membrane. Graphical analyses allow pore-size estimation from permeability measures [45–48, 69, 71–73]. Although the structural substrate of the pathways is probably more complex [48], the "pore" model is a useful functional simplification.

Permeability characteristics

Direct *in vitro* measurements of the biophysical properties of the pleura appear unreliable, because the mesothelium is very labile [6, 20, 52], and the procedures required to obtain the specimens are likely to damage it [6]. Indeed, studies performed on pleura specimens stripped from the underlying tissues [72, 73] provided extremely high values of permeability to water and solutes, which are now regarded as being due to the experimental conditions [28–30, 40–42, 55, 56, 64]. The Lp of the visceral pleura-capillary endothelium membrane obtained *in situ* (0.7–1.0 $\mu L \cdot h^{-1} \cdot cm^{-2} \cdot cmH_2O^{-1}$) [7, 74, 75], is much lower than in stripped pleura [72, 73], but may still be overestimated, because the mesothelium might also have been damaged in these experiments [7, 74]. The Lp of the parietal pleura obtained *in vivo* (1.2 and 2.2 $\mu L \cdot h^{-1} \cdot cm^{-2} \cdot cmH_2O^{-1}$, in dogs and rabbits, respectively) [64] is ~2 orders of magnitude lower than in stripped pleura [72, 73], and slightly greater than Lp of microvascular endothelium [76, 77]. The values, obtained by measurement of convective flows from the pleural space into a capsule glued to the parietal pleura (or to the endothoracic fascia in rabbits), may also be overestimated, because the large (-30 cmH_2O) negative pressure applied to the unsupported interstitium may have stretched the pleura and enlarged the intercellular junctions [6, 42]. Indeed, the low value of σf for albumin (0.3 in dogs and 0.4 in rabbits) computed in the study [64] may reflect albumin transfer through the enlarged intercellular "pores". In another study [78], relatively well-preserved parietal pleura specimens could entertain a $\Delta\pi$ of 24 cmH_2O, suggesting σ to be 0.8–0.9, *i.e.* similar to σ of the visceral pleura (0.93 [75]).

NEGRINI *et al.* [64] also computed P_d to albumin (P_{alb}) of the parietal pleura, obtaining a value of 0.14×10^{-5} $cm \cdot s^{-1}$, >200 times lower than that of stripped pleura [72, 73], and higher than that of muscle, heart and lung capillary endothelium [46, 70]. Restriction to albumin diffusion through the dense connective tissue of the endothoracic fascia (included in the measurement [64]), most likely compensated for the albumin flux through the enlarged junctions. Indeed, the value is similar to P_{alb} directly measured in the mesothelium (0.18×10^{-5} $cm \cdot s^{-1}$ [42]). P_{alb} and P_d of the parietal mesothelium and the underlying connective tissue to various molecules (from H_2O to dextran 2,000 kDa, ranging in radius (a) 0.14–27.9 nm) was obtained from fluxes of labelled molecules across the parietal pericardium [40–43]. Unlike the pleura, this serosa is easily accessible in rabbits, and well-preserved specimens of it can be obtained and studied *in vitro*. The data obtained should apply to the pleura, because cell structure and junction organisation, upon which permeability properties depend [48], are identical in pleura and pericardium [15, 16, 18–22]. Measurements were also carried out after phospholipid (PL) adsorption to the luminal surface, in order to approach more closely the physiological conditions [38, 39]. The mesothelium was found to be responsible for nearly the entire resistance to diffusion through the serosa, the contribution of the connective tissue being negligible despite its 35-times greater thickness. The data provide a complete picture of the permeability properties of the mesothelium, which turned out to be very similar to that of the microvascular endothelium [48]. The graphical analysis devised for the endothelium, applied to the data obtained, allowed estimation of r of mesothelial "pores", as shown in figure 1, a log-log plot of P_d *versus* a.

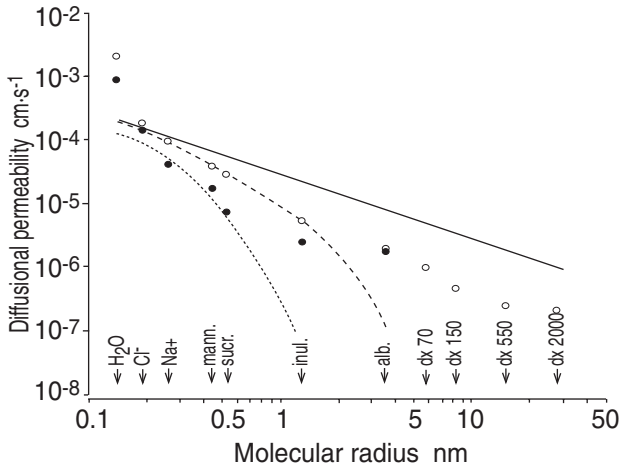

Fig. 1. – Diffusional permeability of mesothelium of parietal pericardium to various solutes *versus* their equivalent radius. Theoretical P-a relationships for free diffusion (—) and for restricted diffusion with 6 (---), and with 1.5 (····) nm "pore" radius are drawn (see text). ○: values obtained without phospholipid adsorption; ●: values obtained after phospholipid adsorption. Sucr.: sucrose; inul.:inulin: alb.: albumin; dx: dextran. Data taken from [40–42].

The line is the theoretical Pd-a relationship for free diffusion (FD), which applies to solutes with a $<\sim$1% r: under FD conditions, Pd is proportional to the solute diffusion coefficient, decreasing with increasing a [45, 69, 71]. Water permeability is greater than predicted by FD through the "pores", suggesting that water also diffuses through cell membranes, like in the endothelium. Support to this hypothesis came from the direct demonstration of aquaporins in pleural mesothelium [79]. PL interact with these channels, as they decrease water permeability (fig. 1). For solutes with a $>\sim$1% r, diffusion is restricted (RD) by friction and steric hindrance with the "pore" walls, and restriction increases with a [45–47, 69–71]: Pd in this range decreases steeply, and the Pd-a relationship is predicted by an equation formulated by RENKIN [45]. The two curves in fig. 1 represent the theoretical Pd-a relationships for RD (obtained by the Renkin equation [45]) which were the best fit for the two sets of data obtained, *i.e.* without (open symbols), and with PL (filled symbols). "Small pore" r was 6 nm without PL, and reduced to 1.5 nm with PL adsorption. These values of r are smaller than the value (8.5 nm) estimated by NEGRINI *et al.* [64], and fit with those of microvascular endothelium [48], and of water-transporting epithelia [41]. P to macromolecules exceeds that expected to occur if they diffused through "small pores" (fig. 1), and Palb is unaffected by the further reduction of r by PL. This means that, as in capillary endothelium [48, 70, 71, 80], macromolecules cannot diffuse through "small pores" (their a being $\geqslant$r), and they follow a different pathway, represented by "large pores" and/or by transcytosis. The same sequence of events affects the Pd-a relationship in the macromolecule range. It initially parallels the FD line (FD through "large pores"); then it becomes progressively steeper (RD through "large pores"). In its last part (d×550-d×2,000), however, it becomes nearly flat, suggesting transcytosis [80]: diffusion stops for macromolecules greater than "large pores", and their transfer occurs by transcytosis, which is independent of a [80]. Transport by transcytosis, which needs to be directly proven, would be in line with the morphological evidence of vesicles in pleural and pericardial mesothelium [15, 16, 18–22, 25]. Experimental support for this was recently provided *in vitro* and *in vivo* (see Liquid exchanges).

Transpleural pressures

Pliq, measured by intrapleural saline-filled cannulae, intercostal capsules, and micropipettes (reviewed in [1–6, 55]), ranges at functional residual capacity (FRC) -1 cmH_2O (in rabbits) to -3 cmH_2O (in dogs) at the bottom of the pleural space in the costal lung region (where Ppl is $\sim$0), and decreases with height by $\sim$1 $cmH_2O \cdot cm^{-1}$. This vertical gradient matches that in Pc, so that the ΔP driving liquid across the pleurae should be independent of height. Pliq decreases with inspiration, and its decrease is greater than that in Ppl. Using an alternative method (rib capsule) instead, Pliq was found to be similar to Ppl, and to undergo vertical gradients <1 $cmH_2O \cdot cm^{-1}$, suggestive of a downward pleural liquid flow [1–6, 55]. With such a vertical gradient, the difference between Pliq and Pc, and, hence, the filtration rate into the pleural space, should decrease with height. Regional differences in Pliq were reported, potentially affecting liquid turnover. 1) Very negative values were measured by long curved cannulae in the mediastinal and diaphragmatic areas [4, 55], where stomas are denser than on the costal surface: this was interpreted as indicating a preferential liquid absorption at these sites, due to parietal lymphatic activity lowering Pliq [55]. However, distortions caused by forcing the cannulae to such a distance may have affected the measurements [4–6]. 2) The mean isoheight Pliq in a breathing cycle is $\sim$5 cmH_2O higher in the costophrenic sinus than in the costal regions facing the lung [81]. This gradient should drive liquid from the costophrenic sinus to the lung zone, *i.e.* in a direction not consistent with stoma distribution. Indeed, this flow suggests that in this area, liquid filtration by Starling forces is greater than lymphatic drainage [81]. In computations of transpleural liquid flows, the average value of Pliq in a breathing cycle should be used, and the considered height should be specified. Values of $\sim$-9, and -6 cmH_2O seem appropriate for the costal region at midlung height in dogs, and rabbits, respectively. In most of the species studied, πliq is $\sim$3–5 cmH_2O [13, 53, 58].

The functional mean Pc at the height of the right atrium of dogs should be $\sim$18 cmH_2O [76] for the parietal pleura capillaries, and $\sim$10 cmH_2O [74, 77] for pulmonary capillaries, both in thin and thick visceral pleura (see Morphological basis of transpleural exchanges); πc should be $\sim$29 cmH_2O.

Measurements of interstitial hydraulic (Pint) and colloidosmotic (πint) pressures are difficult. Pint in the subpleural interstitium of the lung was estimated to be -8 cmH_2O at heart level, with a vertical gradient of

0.7 $cmH_2O \cdot cm^{-1}$ [82]. No direct measure of πint in lung liquid is available in rabbits: that computed from prenodal lymph protein concentration (most likely overestimated, due to the concentration of protein along lymphatics [83]) is 14 cmH_2O [84], while that corresponding to a protein concentration of ~3 $g \cdot dL^{-1}$ [81] is 9–10 cmH_2O. Recently, direct measurements in rabbits with intact pleural space yielded values of -2.4 cmH_2O [85], and -11 cmH_2O [86] for parietal, and visceral Pint, respectively (at a height of 4 cm); and of 11.9 cmH_2O for parietal πint [63]. Pint measurements, however, were made ~200 μm deep to the mesothelium [85, 86]: they, therefore, refer to extrapleural parietal and visceral interstitia, and may not reflect pressures occurring between mesothelium and pleural capillaries, which are only 10–50 μm apart in most species [35]. The value attributed to the visceral pleura [86] pertains to lung parenchyma, because rabbit visceral pleura is <20 μm thick, and the alveoli are only 30–40 μm below the lung surface. The difference should be substantial [6], considering the analysis of the Starling equilibrium by MICHEL [76]: in an interstitium like that of lung parenchyma, which is considered "closed" (*i.e.* only receiving liquid from capillaries [47]), Pint and πint are such that no steady state absorption occurs in its capillaries [76]. Conversely, in an interstitium, like that of the visceral pleura, which is not "closed" because it receives low-protein liquid from the pleural space, Pint should be higher, and πint lower than in lung parenchyma, thus, net liquid absorption should occur at steady state in its capillaries.

Liquid exchanges

Liquid exchanges occur across the pleurae, driven by the above pressures and following other mechanisms as reviewed below. A number of unsolved questions, about the contributions of the various mechanisms to fluid turnover, remain. A tentative schematic representation of the transpleural liquid flows taking place in the rabbit is shown in figure 2.

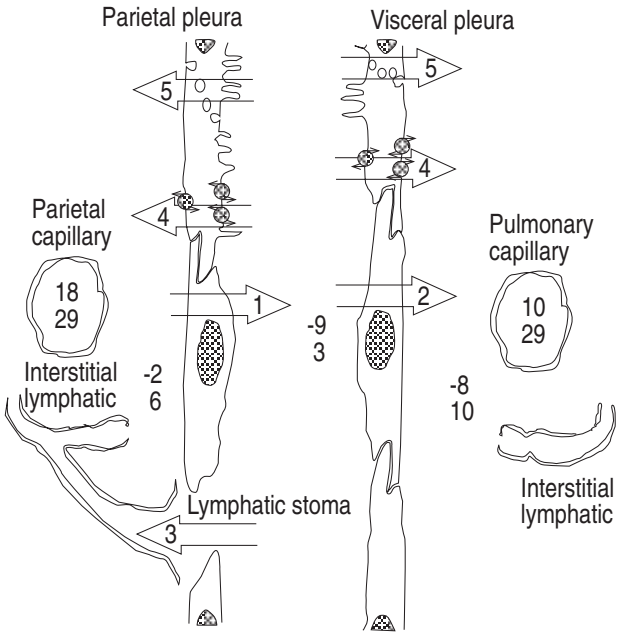

Fig. 2. – Schematic representation of transpleural liquid flows (large arrows) under physiological conditions in rabbit. Mesothelial cells and adjoining interstitia, with embedded capillaries and lymphatics, are shown on each side; the mesothelial cell at the top displays cellular mechanisms involved in pleural liquid turnover (microvilli, vesicles, electrolyte transporters (grey circles)). Arrow size is not proportional to corresponding flow magnitude. 1: Starling filtration at the parietal pleura (tentative estimate: ~0.15–0.20 $mL \cdot h^{-1} \cdot kg^{-1}$); 2: Starling absorption at the visceral pleura (tentative estimate: ~0.1 $mL \cdot h^{-1} \cdot kg^{-1}$); 3: direct drainage through lymphatic stomas (not known; tentative estimate of total pleural lymphatic flow (through stomas+interstitial): ~0.07 $mL \cdot h^{-1} \cdot kg^{-1}$); 4: electrolyte-coupled liquid outflow (measured [30]: 0.07 $mL \cdot h^{-1} \cdot kg^{-1}$); 5: vesicular flow of liquid accompanying protein transcytosis (not known; recent estimates have shown it to be 0.02 $mL \cdot h^{-1} \cdot kg^{-1}$). Pairs of large numbers are hydraulic (above) and colloidosmotic (below) pressures (cmH_2O) involved in Starling balance, pertaining to (from left to right): parietal capillary, parietal interstitium, pleural liquid, visceral interstitium, visceral capillary. Hydraulic pressures refer to heart level; they are functional mean values for capillaries, and averaged value over a breath for pleural liquid, while interstitial values are indirect and uncertain. Interstitial colloidosmotic pressures are uncertain. See text for details, reasons for uncertainty and cautionary comments.

Parietal pleura. It is generally agreed that liquid filters into the pleural space driven by Starling forces through the parietal pleura. Controversies exist on the magnitude of the filtration rate (Jf). The difficulty in estimating Jf is due to the fact that some of the involved parameters are not known with precision, and they display species differences [55]. The computed value of Jf may vary by orders of magnitude depending on the parameters used. Because at equilibrium liquid inflow and outflow must be equal, conclusions on the relative contributions of the different mechanisms to liquid removal are sometimes drawn, based on the estimated Jf, and *vice versa* [17, 67, 87]. These conclusions are obviously affected by large potential errors, and should be taken with caution. Most of the parameters are known for dogs, and a computation may be attempted for this species. With the above-mentioned values of Pc (18 cmH_2O), Pliq (-9 cmH_2O), πc (29 cmH_2O), πliq (~3 cmH_2O), and σ (~0.9), the net filtration pressure through the parietal pleura during a breathing cycle would be ~4 cmH_2O. If Lp is 1.2 $\mu L \cdot h^{-1} \cdot cm^{-2} \cdot cmH_2O^{-1}$ [64], and the parietal pleura surface area is 500 cm^2 [13], Jf in one pleural space of a 9 kg dog would be 0.27 $mL \cdot kg^{-1} \cdot h^{-1}$ (or 4.8 $\mu L \cdot h^{-1} \cdot cm^{-2}$ of parietal pleura). This value should be taken cautiously due to the uncertainties mentioned (and it could be an overestimate, if Lp is overestimated; see Permeability characteristics). Pint (-2.4 cmH_2O [85]) and πint (12 cmH_2O [63]) were used to compute Jf in rabbits [55, 56]. These values, however, may not reflect the relevant ones (see Transpleural pressures), in particular, πint could be lower in the interstitium close to the mesothelium [6]. In fact, no filtration should occur at the parietal pleura in the presence of such values if, as previously found (see above), σ is $\geqslant 0.8$ and πliq ~5 cmH_2O. Only by using a low σ (0.4 [64]; questioned above, see Permeability characteristics, and [6]), together with an abnormally high πliq (8.45 cmH_2O, obtained by refractometry at the end of long experiments

[63]), a small pressure gradient (0.4 cmH_2O) could be computed [55, 56]. The corresponding J_f, computable from the data provided in the same reviews [55, 56], would be $\sim 0.04\ mL \cdot h^{-1} \cdot kg^{-1}$, implying a negligible nonlymphatic outflow from the pleural space (in line with the authors' view). On the other hand, the same author also provided higher J_f values (0.09 and $0.153\ mL \cdot h^{-1} \cdot kg^{-1}$) in the same review [55], and in a contemporary one [54], compatible with a substantial liquid absorption occurring at the visceral pleura. Filtration rate increases with animal size and maturation, [60, 65], and with ventilation, due to a shear stress-induced increase in pleural permeability [5].

Visceral pleura. The ΔP across the visceral pleura is in favour of liquid absorption [1, 2, 4, 6, 55, 56]. Liquid was absorbed according to the Starling forces of the pulmonary capillaries through the visceral pleura in open-chested and perfused dog lungs [7, 74]; the rates of liquid absorption into dog lungs wrapped in water-impermeable membranes changed with the liquid's π, in line with Starling forces [75]. With the above-mentioned values of P_c (10 cmH_2O), P_{liq} (-9 cmH_2O), π_c (29 cmH_2O), π_{liq} ($\sim$3 cmH_2O), and σ ($\sim$0.9), the net absorption pressure through the parietal pleura during a breathing cycle would be $\sim$4 cmH_2O. With such ΔP, if Lp were $0.7\ \mu L \cdot h^{-1} \cdot cm^{-2} \cdot cmH_2O^{-1}$ [7], the absorption rate (J_{visc}) would be $0.18\ mL \cdot h^{-1} \cdot kg^{-1}$ (or $2.8\ \mu L \cdot h^{-1} \cdot cm^{-2}$ of visceral pleura), an overestimation because of the likely overestimated Lp (see Permeability characteristics). The absorption pressure computed when P_{int} and π_{int} are taken into account (see Transpleural pressures) is even larger (7.4 [56], or 8.6 cmH_2O [55]). To reconcile this data with the view that fluid absorption through the visceral pleura is small [17, 55, 56, 67, 87], or negligible [54], it was proposed that Lp of the visceral pleura ought to be very low [56], although no evidence in this direction is provided by the available data (see Permeability characteristics). Considering the uncertainties mentioned, a value of $\sim 0.1\ mL \cdot h^{-1} \cdot kg^{-1}$ in $\sim$2 kg rabbits ($1.8\ \mu L \cdot h^{-1} \cdot cm^{-2}$) could represent a realistic estimate of J_{visc}.

Electrolyte-coupled liquid absorption. Indirect evidence suggests that an electrolyte-coupled liquid absorption contributes to pleural fluid removal in rabbits [8, 28–30, 33]. Such evidence was sought *in vivo* in these studies, because of the delicacy of the mesothelium (see Permeability characteristics). Indeed, no evidence for active transport was found in stripped pleura specimens [72, 73], which were most likely damaged [28–30, 40–42, 55, 56, 64], although the pleural mesothelium displays the features for active transport [25], and an electrical potential difference was found across rat visceral [26], and dog parietal pleura [78]. A luminal Na^+/H^+-Cl^-/HCO_3^- double exchange, and a Na^+-glucose cotransport, coupled to a basolateral Na^+/K^+-ATPase are the mechanisms revealed by the studies [8, 28–30, 33]. Indeed, the flux of Na^+ and the net rate of liquid absorption (J_{net}) were reduced in hydrothoraces containing transport inhibitors (ouabain, bumetanide, amiloride, 4-acetamido-4′-isothiocyanostilbene-2,2′disulphonate, phloridzin) [8, 28, 30, 32, 33]. The reduction ($\sim$40% in hydrothoraces with nearly physiological C_{liq}) increased with protein dilution [30]. It was argued [68] that the effect of amiloride on J_{net} could be due to lymphatic activity inhibition, since amiloride decreased J_{net} and the lymphatic flow from the pleural space in rabbits to the same extent (35%). However, in this study [68] hydrothoraces were large ($\sim$20 times the normal V_{liq}), and some of its results, obtained after prolonged anaesthesia (3 h, previously shown to affect pleural liquid turnover [88]) are conflicting, as previously pointed out [6, 89]. On the other hand, evidence in favour of active transport in the pleural mesothelium was also obtained without inhibitors: liquid flow reversed when Na^+, or Cl^- in the hydrothorax were substituted by impermeant solutes [28]; Na^+ concentration decreased in hypertonic hydrothoraces (containing mannitol $30\ mM \cdot L^{-1}$), because water could not follow the transported Na^+ [29]. Furthermore, the decrease in J_{net} caused by inhibitors in hydrothoraces of increasing size (0.5–5 mL) is independent of V_{liq}, in line with the inhibition of an active transport [30–33], while lymphatic drainage should increase with V_{liq} [53]. Similar to what is found in alveolar epithelium [90], the active transport is enhanced by β_2-receptor stimulation [31, 32, 34], which causes a concomitant depression of lymphatic drainage [91]. The solute-coupled liquid outflow ($J_{s\text{-}c}$) should occur on both pleurae, opposing filtration on the parietal, and enhancing absorption on the visceral side [8]. $J_{s\text{-}c}$ under physiological conditions amounts to $\sim 0.07\ mL \cdot h^{-1} \cdot kg^{-1}$ ($\sim 0.7\ \mu L \cdot h^{-1} \cdot cm^{-2}$ of pleura).

Lymphatic drainage. The lymphatic flow from the pleural space (J_l) under nearly physiological conditions amounts to $0.02\ mL \cdot h^{-1} \cdot kg^{-1}$ [67, 87], ($\sim 0.4\ \mu L \cdot h^{-1} \cdot cm^{-2}$ of parietal pleura), as computed in dogs from the egress kinetics of labelled albumin injected into the space in a 0.5 mL bolus. Considering that this value is underestimated, according to the authors [67], and that in rabbits the turnover rate is greater than in dogs, a J_l of $\sim 0.07\ mL \cdot h^{-1} \cdot kg^{-1}$ may be estimated to occur in rabbits. It should be noted, however, that this represents the overall lymphatic flow from the pleural space, inclusive of that provided by interstitial lymphatics, which drain some of the albumin (and liquid) transported across the pleurae outside the stomas (solvent drag, transcytosis; [4]). Hence, the direct lymphatic flow through the stomas ($J_{l,s}$) only accounts for a part of J_l. Therefore, the marked reduction in the amount of labelled albumin reaching the blood after ligation of the right lymphatic or thoracic duct [67] does not prove that $J_{l,s}$ accounts for most of liquid removal, but simply shows that albumin is drained by lymphatics (including interstitial ones) [4]. The exact contributions of the other pathways (solvent drag, diffusion, transcytosis) to protein transpleural transfer need to be determined in order to assess $J_{l,s}$. $J_{l,s}$ is essential to remove particles and cells [53] from the pleural space, it increases with C_{liq} [30, 88, 92], with stimulation of lymphatic smooth muscle β_2-receptors [34], and, most importantly, with increased V_{liq} [53, 68, 88]. Under this condition $J_{l,s}$ represents the most effective means of limiting further liquid accumulation, and it becomes the main mechanism of liquid outflow, up to its

saturation [54–56] (see Pathophysiology of pleural fluid turnover).

$J_{l,s}$ is considered by some to be the main path of liquid outflow from the pleural space, even under physiological conditions [3, 5, 17, 54–56, 94]. On the other hand, most available information and a number of considerations argue against this view. A role for the visceral pleura in pleural fluid turnover was dismissed, on the basis of the contention that the mesothelium is leaky [94], or nearly impermeable [54–56], or that no pressure gradients exist for liquid absorption through it [94]. As noted above (see Permeability characteristics), direct and indirect evidence supports the notion that the pleural mesothelium is not as leaky as it was previously thought: its permeability to water and solutes is comparable to that of capillary endothelium, it entertains a protein concentration gradient, and it appears to actively transport solutes and liquid [8, 15, 19, 25, 28–30]. Net absorptive pressure gradients are computed across the visceral pleura [1, 2, 4, 6, 55, 56], and, the Jf and Jvisc values computable from these gradients and the permeability parameters (see Liquid exchanges) are greater (up to one order of magnitude) than available estimates of pleural lymphatic flow under physiological conditions [67, 87]. It was maintained that the absorption of nearly protein-free liquid through the lung surface should lead to a progressive increase in C_{liq} [17], but a protein balance analysis of the pleural space [4] (also taking into account protein fluxes by solvent drag) showed that, on the contrary, C_{liq} may remain constant and low even if $J_{l,s}$ is less than nonlymphatic liquid absorption. Furthermore, the experimental evidence presented as supporting a predominant role of $J_{l,s}$ in pleural liquid removal [54–56, 93] is far from conclusive. 1) Liquid absorption from hydrothoraces was found to be independent of π_{liq} [88, 95], but in similar experiments it was found that J_{net} decreased with increasing π_{liq}, and it became nil with serum, plasma or 5% albumin-Ringer hydrothoraces [92]. 2) It was concluded that liquid is preferentially absorbed from areas where stomas are denser, because intrapleurally injected labelled albumin appeared (by gamma camera scannings) to mostly decay from mediastinal, diaphragmatic, and apical regions of dog pleural space [67], but apical regions do not contain stomas [18, 19], and part of the measured activity could be due to albumin transferred across the visceral pleura, and eventually removed by lung lymphatics [4, 6], not by parietal stomas. Similar considerations, as already observed, apply to the conclusions drawn by MINIATI *et al.* [87]. 3) The absorption of liquid at negative pressure from a capsule glued to the peritoneal side of the diaphragmatic tendon [96], presented as the effect of drainage by peritoneal diaphragmatic lymphatics, can also interpreted as passive convection driven by the pressure gradient imposed [96] through the diaphragm [6].

It was hypothesised that parietal pleura lymphatics are able to decrease P_{liq} by their pumping activity [55]. The negligible surface area of the stomas compared to that of the pleura [18, 19], argues against this hypothesis [5] (though stomas are 100 time more dense in mice [51], and their area increases during inspiration [50]). Conversely, parietal pleura lymphatics (like those of lung interstitium, and of any interstitia) should be able to drain liquid at a slightly lower pressure than that of their ambient. Indeed, their intraluminal pressure (P_{lymph}) may be lowered by extrinsic distending forces, acting in the tissue in which they are embedded (*e.g.* tensile stress undergone by diaphragmatic fibres for diaphragmatic lymphatics [93]; lung recoil and interdependence forces for lung lymphatics [2, 6]). Liquid at subatmospheric pressure fills the lymphatic lumen when, upon release of compressive forces, lymphatics recoil under the effect of distending forces. Compressive forces, both extrinsic (*e.g.* respiratory muscle contraction during spontaneous breathing, or transmission of cardiogenic oscillation) and intrinsic (lymphatic smooth muscle contraction), increase P_{lymph}, propelling lymph through unidirectional valves. P_{lymph} in parietal pleural lymphatics was recently measured in paralysed rabbits at FRC [93]. Baseline P_{lymph} was -0.17 kPa (-1.3 mmHg) in intercostal vessels (*i.e.* less negative than isoheight P_{liq} [93]), and -2.13 kPa (-16 mmHg) in diaphragmatic lymphatics in the costophrenic sinus (*i.e.* markedly lower than isoheight P_{liq}, simultaneously measured in the costal lung zone, -0.52 kPa (-3.9 mmHg) [93], or than P_{liq} previously measured in the costophrenic sinus, $\sim$-10 cmH_2O [81]). Tensile stress transmitted from diaphragmatic fibres is thought to cause this low pressure [93]. Cardiac oscillations caused pulsatile increases in P_{lymph} of $\sim$0.67 kPa (5 mmHg), and myogenic lymphatic contractions produced increases of $\sim$0.93 kPa (7 mmHg).

Transcytosis. Vesicular transport of liquid, associated with protein transcytosis, represents an additional pathway for pleural liquid absorption, as recently shown [97, 98], and in line with morphological evidence of cytoplasmic vesicles [15, 16, 18–22, 25] and with indirect physiological evidence ([42]; see Permeability characteristics). Transcytosis of macromolecules from the luminal to the interstitial side of the mesothelium was directly demonstrated to occur in parietal pericardial specimens *in vitro* [97]. More recently, in *in vivo* experiments on rabbits, nocodazole, an inhibitor of transcytosis, was shown to markedly reduce the absorption of labeled macromolecules injected into the pleural space, and their appearance in circulating plasma [98]. It was computed that transcytosis removed $\sim$160 $\mu g \cdot h^{-1} \cdot kg^{-1}$ (1.8 $\mu g \cdot h^{-1} \cdot cm^{-2}$) of albumin from the pleural space, and 18 $\mu L \cdot h^{-1} \cdot kg^{-1}$ (0.2 $\mu L \cdot h^{-1} \cdot cm^{-2}$ of pleura) of liquid [98]. This albumin is then transported by interstitial lymphatics contributing substantially to the overall lymphatic drainage of albumin and liquid (see Lymphatic drainage). These new data [97, 98] suggest a relevant role for protein transcytosis in the control of pleural fluid colloidosmotic pressure, and in pleural fluid turnover. On the other hand, they show that $J_{l,s}$ is not the only pathway for protein removal from the pleural space, and that its role in pleural fluid turnover seems to have been overemphasised.

Pathophysiology of pleural-fluid turnover

Hydrothorax dynamics

An increase in pleural liquid volume *per se* represents a limiting factor of further accumulation of liquid, entailing changes in the balance of transpleural forces and increasing lymphatic drainage, which shift the balance of liquid flows towards net absorption [1, 2, 55, 56]. The effect of these mechanisms, providing a sort of negative feedback control, may be observed in animals with artificially induced hydrothoraces, where no alterations of the factors involved in pleural fluid turnover pre-exist [1, 2, 8, 28–34, 53, 61, 68, 88, 92, 95]. With increased V_{liq}: 1) P_{liq} increases, reducing ΔP across the parietal pleura, while increasing that across the visceral pleura; 2) if the hydrothorax is performed with protein-free fluid [1, 2, 8, 28–30, 68, 95], the reduced π_{liq} effects similar changes; 3) the increase in V_{liq} *per se*, and the associated increase in P_{liq} (favouring initial lymphatic filling, and enhancing the contractility of lymphatic smooth muscle), causes an increase in $J_{l,s}$ [53, 68, 88, 95]. $J_{s\text{-}c}$, on the other hand, does not change with V_{liq} [30]. The effect of the increased P_{liq} should be greater with small hydrothoraces. Indeed, P_{liq} rises steeply with the first liquid volume injected (which releases the deformation forces between lung and chest wall), while it increases less steeply, becoming almost constant with the introduction of further liquid [2]. This smaller increase is related to lung volume decreasing in the dependent parts of the space, where contact between lung and chest wall is lost due to liquid accumulation [1, 2]. $J_{l,s}$ increases markedly when V_{liq} or P_{liq} increase [53, 68, 88], the increase extending to rather large liquid loads, and is probably the main outflow mechanism operating with large effusions, becoming >20-times greater than the physiological value in 10 $mL \cdot kg^{-1}$ hydrothoraces (>100 times the normal V_{liq}) in sheep [53]. The effect of hydrothorax size on the joint contribution of Starling forces and lymphatic drainage to liquid absorption may be inferred from the relationship between J_{net} and hydrothorax size found in rabbits with artificial hydrothoraces of increasing volume (0.2–2.3 $mL \cdot kg^{-1}$, *i.e.* 3–21 times the physiological volume) containing amiloride (*i.e.* after removing the contribution by $J_{s\text{-}c}$) [30]. With nearly physiological C_{liq} (~1.3 $g \cdot dL^{-1}$), liquid absorption increased steeply (from 0.03 to 0.12 $mL \cdot kg^{-1} \cdot h^{-1}$) up to a V_{liq} of ~1 $mL \cdot kg^{-1}$, then it increased less, reaching 0.17 $mL \cdot kg^{-1} \cdot h^{-1}$ with the largest hydrothorax. The initial steeper slope should reflect the combined increase in Starling absorption and $J_{l,s}$ with small liquid loads, while its last part should reflect the progressive increase in $J_{l,s}$ with larger loads [30]. By transferring to humans the values measured in animals, it was calculated that J_l could increase in man from ~34 $mL \cdot day^{-1}$ (2% of the overall lymph flow) to ~700 $mL \cdot day^{-1}$ (40% of the overall lymph flow) [54]. In rabbits with a 2.2 $mL \cdot kg^{-1}$ hydrothorax, J_l was 0.58 $mL \cdot kg^{-1} \cdot h^{-1}$, as estimated from the clearance rate of labelled lactate dehydrogenase (LDH) [68]. In these rabbits, the volume in the contralateral pleural space was also increased (by ~3 times), and the computed J_f was high (0.41 $mL \cdot kg^{-1} \cdot h^{-1}$) [68]. Similar results had been obtained in dogs in a pioneering study by STEWART and BURGEN [99], in which pleural inflammation is suspected to have occurred [61], on the basis of a very high cell count in pleural fluid (40,000–50,000 μL^{-1}). In sheep with a 10 $mL \cdot kg^{-1}$ hydrothorax, the removal rate was 0.28 $mL \cdot kg^{-1} \cdot h^{-1}$, and $J_{l,s}$, estimated from the clearance rate of labelled red blood cells, accounted for 89% of it [53]. It should be noted that with such large hydrothoraces, leading to high P_{liq}, a substantial amount of protein (7% in 15 min [53]) is driven by solvent drag through the mesothelium: this amount, eventually removed by interstitial lymphatics, should not be included in computations to estimate $J_{l,s}$ [53].

Pleural effusions

When the increase in V_{liq} is sustained by altered pleural liquid turnover (pleural effusion), *i.e.* when the filtration rate exceeds the potential for increased absorption, or when one of the absorbing mechanisms is primarily altered, the compensatory mechanisms are bound to be overwhelmed; in particular, maximum J_l may be reached, with saturation of the lymphatic mechanism [55, 56]. Recovery from large effusions will only become possible when the Starling pressure balance, lymphatic drainage and/or permeability characteristics return to normal. Several conditions may disturb the equilibrium of forces involved in fluid transfer across the pleurae, leading to an imbalance between the rate of fluid formation and that of fluid reabsorption. Extensive reviews on the pathophysiology of pleural effusions are available [100–104]. The causes of pleural effusion may be subdivided into three main categories: 1) those changing transpleural pressure balance, 2) those impairing lymphatic drainage, and 3) those producing increases in mesothelial and capillary endothelial permeability. Factors altering the balance of Starling forces are generally extrapleural in nature, those decreasing lymphatic drainage may primarily involve either pleural, or extrapleural lymphatics, while those causing loss of membrane selectivity obligatorily involve the pleural mesothelium. Except in the first case, C_{liq} increases above normal: this feature underlies the classification of pleural effusions into transudative (with normal C_{liq}), and exudative. In the clinical setting, separation of transudates from exudates is generally achieved by the criteria presented by LIGHT *et al.* [104]: exudates have C_{liq}/C_c >0.5, pleural liquid/serum LDH >0.6, or pleural liquid LDH >2/3 of the upper limit of the normal value for serum. Besides revealing loss of pleural selectivity to macromolecules, these criteria disclose the inflammation often accompanying exudates. Indeed, cellularity is often increased in exudates [24, 106]. When compared to other proposed tests, the classical criteria have been confirmed as the most reliable in the task [107]. One alternative test, however (C_{liq} differing from protein concentration in serum by >1.2 $g \cdot dL^{-1}$ [108]), seems useful [107] in revealing the true nature of an effusion if a transudate is apparently

transformed into an exudate due to preferential fluid absorption during acute diuretic therapy [109].

Transudates. Increases in the capillary and mesothelial Kf values may occur [54], although possibly of lesser clinical interest; they could contribute to the initial (transudative) stages of effusions associated with inflammatory processes. Indeed, an increase in the capillary Kf, not accompanied by changes in σ to protein occurs with heating, histamine-like mediators and calcium ionophores (reviewed in [48]). Increases in systemic capillary pressure increase the rate of filtration at the parietal pleura. The resulting C_{liq} is reduced relative to normal, if the sieving properties of the capillaries and mesothelium are preserved. Indeed, C_{liq} is smaller, and θ greater in spontaneously hypertensive rats (in which P_c was estimated to be ~3.9 kPa (30 mmHg)), relative to age-matched controls [65]. Systemic venous hypertension also affects lymphatic drainage, which is hindered by an elevation of the outflow pressure at the thoracic duct [100–103]. Increases in pulmonary capillary pressure hinder fluid absorption at the visceral pleura, and may reverse the net pressure gradient, causing liquid filtration to occur from the lung surface. Pulmonary venous hypertension seems to be the main cause of pleural effusion in cardiac disease [110, 111]: patients with congestive heart failure and pleural effusion have higher pulmonary capillary wedge pressure than patients without effusion, while right atrial pressure is not significantly different between the two groups [110]. Isolated right ventricular failure or chronic pulmonary hypertension was not found to be associated with pleural effusions [111]. In an older study [59], systemic venous hypertension was found to cause greater pleural fluid accumulation than pulmonary venous hypertension in dogs. This was attributed to a greater Kf and surface area of systemic, relative to pulmonary capillaries. However, the concomitant low value of π_c (due to saline infusion [59]) also affected pleural fluid turnover, preventing clear interpretation of the findings of this study [2, 112]. Pleural effusion was found to occur with both hydrostatic [113, 114] and increased permeability lung oedema [113, 115]. Leak of oedema fluid into the pleural space was suggested to represent an important route of interstitial oedema clearance, acting as a safety factor with regard to alveolar flooding [112]. While agents causing high-permeability oedema are likely to also affect pleural permeability, in pure hydrostatic oedema the mesothelial barrier properties should be retained, and protein-rich effusions are rare in pulmonary oedema in man [54]. On the other hand, the effusions occurring in volume loading experiments on *in situ* isolated lungs in sheep were exudates, C_{liq} being similar to protein concentration in lung oedema fluid [113]: this implies that the barrier properties of the capillary-mesothelium membrane were altered in these experiments [54]. Furthermore, MISEROCCHI *et al.* [115] did not find evidence of increased V_{liq} in rabbits with lung interstitial oedema over a 3-h period of observation, despite an increase in P_{int} to ~6 cmH_2O. Therefore, increases in capillary surface area, and in pleural Lp, associated with pulmonary vascular congestion and inflammation were hypothesised to justify filtration through the visceral pleura [54]. Less frequent causes of transudates due to increased P_c are constrictive pericarditis, fluid overload in critical patients, hypervolaemia associated with chronic renal failure (reviewed in [100–104]). The latter conditions may also act by altering π_c. Hypoalbuminaemia *per se*, however, was recently proven to be an uncommon cause of pleural effusion in a combined prospective and retrospective study [116]. Indeed, pleural effusion only occurred in 14%, and in 4% of the study patients with albuminaemia of 1.8, and 3.0 $g \cdot dL^{-1}$, respectively; furthermore, alternative explanations for the pleural effusion were identified in most of the patients presenting it [116]. Indeed, it is likely that chronic hypoalbuminaemia affects the protein balance across the pleura, such that the change in π_c is offset by a concomitant decrease in π_{liq}. A decreased P_{liq}, resulting from prevention of lung expansion, may also unbalance ΔP in favour of filtration: this may occur in the case of atelectasis, or with the "trapped lung" following formation of a fibrous peel over the lung, as a consequence of inflammation [100–104]. An exudate-like transformation generally occurs due to associated impairment of lymphatic absorption [100].

Transudate-like fluid may also accumulate in absence of altered pleural liquid turnover, by entering the pleural space through nonphysiological routes: pleuro-peritoneal communications through microscopic diaphragmatic defects provide the pathway through which peritoneal dialysis, or ascitic fluid may be driven by the favourable pressure gradient between abdomen and pleural space [117]. This occurs in some cases of hepatic cirrhosis, occasionally even in absence of visible ascites. Other causes were hypothesised for pleural effusion in hepatic disease (hypoproteinaemia, azygous hypertension [100, 103], but studies with labelled albumin confirmed the peritoneal origin of the fluid [117]. Passage through the diaphragmatic lymphatic network has also been hypothesised [100].

Exudates. Exudates form when protein and cell removal from the pleural space is impaired, or when protein (and cells) enter the pleural space through a leaky mesothelial membrane. Impairment of lymphatic drainage may be a primary cause of an exudate. Indeed, besides its contribution to liquid removal, a normal $J_{l,s}$ is crucial in keeping a low π_{liq}, since it contributes to remove protein from the pleural space. When π_{liq} increases, the balance of pressures across the pleurae is altered, favouring filtration and further hindering absorption. The effusion, often a transudate in its early stages [101], soon becomes an exudate, even in absence of altered barrier permeability characteristics. Decreased lymphatic flow may follow direct involvement of the pleural lymphatics, as with pleural infiltration by infectious processes or malignancy [100–104], and stoma blockage by fibrin deposition in the later stages of parapneumonic effusions [104]; or result from extrapleural lymphatic alterations, as in hypoplasia of the lymphatic system, obstruction of mediastinal lymphatics or of the thoracic duct [100–104]. Increased systemic venous pressure may

also reduce J_l by increasing the outflow pressure in the thoracic duct [100–103].

Increased microvascular and mesothelial permeability typically underlie the occurrence of most exudates. The mechanisms of increased microvascular permeability have been extensively studied, and the available knowledge allowed identification of one of its key processes in cytoskeletal function [48]; progress in understanding its features is going to result from investigation of the modulation of actomyosin interaction by various inflammatory stimuli. Review of the mechanisms of increased microvascular permeability is beyond the scope of this article: the reader is referred to the recent review by MICHEL and CURRY [48]. Microvascular permeability increases by two modalities: opening of new gaps between cells, possibly consequent to cells contracting away from each other, or opening of transcellular pathways, possibly by fusion of cytoplasmic vesicles with the cell membrane. In the first case, "pore" area increases without changes in r, *i.e.* permeability to water and small solutes is greater, but leakage of macromolecules is still restrained; in the second case, permeability to macromolecules is also increased. A range of stimuli and mediators have been found to cause these effects in endothelium [48]. The mesothelium may share some of the mechanisms, since some of the mediators, known to be involved in altered microvascular permeability are found in pleural exudates. The origin of these mediators may either be extrapleural, or from the pleural mesothelium itself, since activated mesothelial cells release a variety of chemokines, cytokines and growth factors, all of which may affect permeability, and may become actively phagocytic, releasing oxidants and proteases and expressing cell-surface molecules (reviewed in [23, 24, 106]). In turn, this affects influx into the pleural space of a variety of inflammatory cells, which also produce mediators furthering the alterations of the mesothelial barrier. Cellular mechanism, most likely differentiated according to the primary abnormality, are thought to be implicated in the genesis of exudates associated with all forms of local inflammation (pulmonary infection, embolism, pleuritis in systemic collagen diseases), and in malignancies, often in association with impaired J_l due to direct involvement of pleural or mediastinal lymphatics.

The events leading to the formation of an inflammatory exudate were defined for the effusions associated with pulmonary infection (parapneumonic effusion) [104], the most frequent form of exudate, and they likely operate in the case of any subpleural inflammation (including those occurring in proximity to the parietal pleura, as in chronic pericarditis, pancreatitis, subphrenic abscesses). During inflammation of subpleural alveolar areas [104], protein-rich fluid leaks into lung interstitium (due to vasodilation and increased P_c, and to increased endothelial permeability). The increased P_c and P_{int}, although opposed by the increased π_{int}, result in a net filtering pressure across the visceral pleura, and should cause a transudate-like effusion if the mesothelium retains its sieving properties. This situation, however, is only temporary, because soon inflammatory cells and mediators interact with mesothelial cells. Direct mesothelial damage with loss of barrier selectivity occurs, and a small, PMN predominant, but sterile exudate, ensues (capillary leak or exudative stage). In a further stage, if endothelial and mesothelial injury aggravate, pleural fluid formation increases, bacteria may enter the pleural space (bacterial invasion/fibrinopurulent stage), and deposition of a dense layer of fibrin on both pleural surfaces occurs, further increasing permeability, and impeding fluid removal. Indeed, a disordered fibrin turnover occurs in the pleural space in association with exudates, involving increased procoagulant and depressed fibrinolytic activity (interestingly, opposite changes are found in transudates) [118].

Conclusions

A number of mechanisms interact in controlling the volume and composition of the liquid contained in the pleural space, thus contributing to maintain the conditions for an efficient mechanical coupling between chest wall and lung. In addition to the long known relevance of the balance of pressures across the mesothelium and of the lymphatic drainage, the importance of the mesothelium in controlling transpleural exchanges is revealed by recent physiological studies, in line with morphological evidence and with recent studies on the biological characteristics of the normal and diseased pleural mesothelial cell. The study of the cellular mechanisms affecting pleural liquid composition seems to be most promising in elucidating the mechanisms of pleural liquid turnover in normal and abnormal conditions.

References

1. Agostoni E. Mechanics of the pleural space. *Physiol Rev* 1972; 52: 57–128.
2. Agostoni E. Mechanics of the pleural space. *In*: Macklem PT, Mead J, eds. Handbook of Physiology: The Respiratory System, Mechanics of Breathing. Baltimore, American Physiological Society, 1986; pp. 531–559.
3. Lai-Fook SJ, Rodarte JR. Pleural pressure distribution and its relationship to lung volume and interstitial pressure. *J Appl Physiol* 1991; 70: 967–978.
4. Agostoni E, D′Angelo E. Pleural liquid pressure. *J Appl Physiol* 1991; 71: 393–403.
5. Lai-Fook SJ, Wang PM. Dynamics of pleural liquid. *In*: Hlastala MP, Robertson HT, eds. Complexity in Structure and Function of the Lung. New York, Dekker, 1997; pp. 123–149.
6. Agostoni E, Zocchi L. Mechanical coupling and liquid exchanges in the pleural space. *Clin Chest Med* 1998; 19: 241–260.
7. Agostoni E, Taglietti A, Setnikar I. Absorption force of the capillaries of the visceral pleura in determination of the intrapleural pressure. *Am J Physiol* 1957; 191: 277–282.
8. Agostoni E, Zocchi L. Solute-coupled liquid absorption from the pleural space. *Respir Physiol* 1990; 81: 19–27.

9. Lai-Fook SJ, Beck KC, Southorn PA. Pleural liquid pressure measured by micropipettes in rabbits. *J Appl Physiol* 1984; 56: 1633–1639.
10. Lai-Fook SJ, Kaplowitz M. Pleural space thickness in situ by light microscopy in five mammalian species. *J Appl Physiol* 1985; 59: 603–610.
11. Wang PM, Lai-Fook SJ. Upward flow of pleural liquid near lobar margins due to cardiogenic motion. *J Appl Physiol* 1992; 73: 2314.
12. Butler JP, Huang J, Loring SH, *et al.* Model for a pump that drives circulation of pleural fluid. *J Appl Physiol* 1995; 78: 23–29.
13. Miserocchi G, Agostoni E. Contents of the pleural space. *J Appl Physiol* 1971; 30: 208–213.
14. Albertine KM, Wiener-Kronish JP, Roos PJ, Staub NC. Structure, blood supply, and lymphatic vessels of the sheep visceral pleura. *Anat Rec* 1982; 165: 277–294.
15. Jaurand MC, Fleury-Feith J, Bernaudin JF, Bignon J. Pleural mesothelial cells. *In*: Crystal RG, West JB, eds. The Lung: Scientific Foundations. Philadelphia, Raven, 1997; pp. 961–969.
16. Mariassy AT, Wheeldon EB. The pleura: a combined light microscopic, scanning and transmission electron microscopic study in the sheep. 1. Normal pleura. *Exp Lung Res* 1983; 4: 293–313.
17. Staub NC, Wiener-Kronish JP, Albertine KH. Transport through the pleura. *In*: Chrétien J, Bignon J, Hirsch A, eds. The Pleura in Health and Disease. New York, Dekker, 1985; pp. 169–193.
18. Wang N-S. The regional difference of pleural mesothelial cells in rabbits. *Am Rev Respir Dis* 1974; 110: 623–633.
19. Wang N-S. Anatomy of the pleura. *Clin Chest Med* 1998; 19: 229–240.
20. Fentie IH, Allen DJ, Schenck MH, Didio LJA. Comparative electron-microscopic study of bovine, porcine, and human parietal pericardium as materials for cardiac valve bioprostheses. *J Submicrosc Cytol* 1986; 18: 53–65.
21. Ishihara T, Ferrans VJ, Jones M, Boyce SW, Kawanami O, Roberts WC. Histologic and ultrastructural features of normal human parietal pericardium. *Am J Cardiol* 1980; 46: 744–753.
22. Thomas NW. Embryology and structure of the mesothelium. *In*: Jones JS, ed. Pathology of the Mesothelium. New York, Springer-Verlag, 1987; pp. 1–13.
23. Antony VB, Sahn SA, Mossman B, Gail DB, Kalica A. Pleural cell biology in health and disease. *Am Rev Respir Dis* 1992; 145: 1236–1239.
24. Kroegel C, Antony VB. Immunobiology of pleural inflammation: Potential implications for pathogenesis, diagnosis and therapy. *Eur Respir J* 1997; 10: 2411–2418.
25. Gil J. Morphological basis of exchanges across the pleura. *In*: Chrétien J, Bignon J, Hirsch A, eds. The Pleura in Health and Disease. New York, Dekker, 1985; pp. 88–99.
26. Engelberg J, Radin J. Tracheal-vascular and vascular-pleural potential in the rat lung. *Respir Physiol* 1977; 30: 253–263.
27. Schröppel B, Fischereder M, Wiese P, Segerer S, Huber S. Expression of glucose transporters in human peritoneal mesothelial cells. *Kidney Int* 1998; 53: 1278–1287.
28. Zocchi L, Agostoni E, Cremaschi D. Electrolyte transport across the pleura of rabbits. *Respir Physiol* 1991; 86: 125–138.
29. Zocchi L, Cremaschi D, Agostoni E. Liquid volume, Na^+ and mannitol concentration in a hypertonic mannitol-Ringer hydrothorax. *Respir Physiol* 1992; 89: 341–351.
30. Agostoni E, Zocchi L. Active Na^+ transport and coupled liquid outflow from hydrothoraces of various size. *Respir Physiol* 1993; 92: 101–113.
31. Zocchi L, Agostoni E. Effect of β-adrenergic blockade or stimulation on net rate of hydrothorax absorption. *Respir Physiol* 1994; 97: 347–356.
32. Zocchi L, Agostoni E, Cremaschi D. β-agonist activation of an amiloride-insensitive transport mechanism in rabbit pleura. *Respir Physiol* 1995; 1007–13.
33. Zocchi L, Agostoni E, Raffaini A. Effect of phloridzin on net rate of liquid absorption from the pleural space of rabbits. *Exp Physiol* 1996; 81: 957–967.
34. Zocchi L, Raffaini A, Agostoni E. Effect of adrenaline on net rate of liquid absorption from the pleural space of rabbits. *Exp Physiol* 1997; 82: 507–520.
35. Bernaudin J-F, Fleury J. Anatomy of the blood and lymphatic circulation of the pleural serosa. *In*: Chrétien J, Bignon J, Hirsch A, eds. The Pleura in Health and Disease. New York, Dekker, 1985; pp. 23–42.
36. Andrew PM, Porter KR. The ultrastructural morphology and possible functional significance of mesothelial microvilli. *Anat Rec* 1973; 177: 409–426.
37. Madison LD, Bergstrom-Porter B, Torres AR, Shelton E. Regulation of surface topography of mouse peritoneal cells. *J Cell Biol* 1979; 82: 783–797.
38. Hills BA, Butler BD, Barrow RE. Boundary lubrication imparted by pleural surfactants and their identification. *J Appl Physiol* 1982; 53: 463–469.
39. Hills BA, Butler BD. Phospholipids identified on the pericardium and their ability to impart boundary lubrication. *Ann Biomed Engineer* 1985; 13: 573–586.
40. Zocchi L, Raffaini A, Agostoni E, Cremaschi D. Diffusional permeability of rabbit mesothelium. *J Appl Physiol* 1998; 85: 471–477.
41. Agostoni E, Bodega F, Zocchi L. Equivalent radius of paracellular "pores" of the mesothelium. *J Appl Physiol* 1999; 87: 538–544.
42. Bodega F, Zocchi L, Agostoni E. Macromolecule transfer through mesothelium and connective tissue. *J App Physiol* 2000; 89: 2165–2173.
43. Bodega F, Zocchi L, Cremaschi D, Agostoni E. Electrical resistance and ion diffusion through mesothelium. *Respir Physiol* 2001; 124: 231–241.
44. Hills BA. The Biology of Surfactant. Cambridge, Cambridge University Press, 1988.
45. Renkin EM. Filtration, diffusion, and molecular sieving through porous cellulose membranes. *J Gen Physiol* 1954; 38: 225–243.
46. Renkin EM. Multiple pathways of capillary permeability. *Circ Res* 1977; 41: 735–743.
47. Levick JR. An Introduction to Cardiovascular Physiology. London, Butterworths, 1991.
48. Michel CC, Curry FE. Microvascular permeability. *Physiol Rev* 1999; 79: 703–761.
49. Wang N-S. The preformed stomas connecting the pleural cavity and the lymphatics in the parietal pleura. *Am Rev Respir Dis* 1975; 111: 12–20.
50. Negrini D, Mukenge S, Del Fabbro M, Gonano C,

Miserocchi G. Distribution of lymphatic stomata. *J Appl Physiol* 1991; 70: 1544–1549.
51. Kanazawa K. Exchanges through the pleura. Cells and particles. *In*: Chretien J, Bignon J, Hirsch A, eds. The Pleura in Health and Disease. New York, Dekker, 1985; pp. 195–231.
52. Peng MJ, Wang NS, Vargas FS, Light RW. Subclinical surface alterations of human pleura. A scanning electron microscopic study. *Chest* 1994; 106: 351–353.
53. Broaddus VC, Wiener-Kronish JP, Berthiaume Y, Staub NC. Removal of pleural liquid and protein by lymphatics in awake sheep. *J Appl Physiol* 1988; 64: 384–390.
54. Miserocchi G. Physiology and pathophysiology of pleural fluid turnover. *Eur Respir J* 1997; 10: 219–225.
55. Miserocchi G, Negrini D. Pleural space: pressure and fluid dynamics. *In*: Crystal RG, West JB, eds. The Lung: Scientific Foundations. Philadelphia, Lippincott-Raven, 1997; pp. 1217–1225.
56. Negrini D. Integration of capillary, interstitial and lymphatic function in the pleural space. *In*: Reed RK, Mc Hale NG, Bert JL, eds. Interstitium Connective Tissue and Lymphatics. London, Portland, 1995; pp. 283–299.
57. Broaddus VC, Araya M. Liquid and protein dynamics using a new minimally invasive pleural catheter in rabbits. *J Appl Physiol* 1992; 72: 851–857.
58. Sahn SA, Willcox ML, Good JT Jr, Potts DE, Filley GF. Characteristics of normal rabbit pleural fluid: physiologic and biochemical implications. *Lung* 1979; 156: 63–69.
59. Mellins RB, Levine OR, Fishman AP. Effect of systemic and pulmonary venous hypertension on pleural and pericardial fluid accumulation. *J Appl Physiol* 1970; 29: 564–569.
60. Broaddus VC, Araya M, Carlton D, Bland RD. Developmental changes in pleural liquid protein concentration in sheep. *Am Rev Respir Dis* 1991; 143: 38–41.
61. Wiener-Kronish JP, Albertine KH, Licko V, Staub NC. Protein egress and entry rates in pleural fluid and plasma in sheep. *J Appl Physiol* 1984; 56: 459–463.
62. Noppen M, DeWaele M, Li R, *et al.* Volume and cellular content of normal pleural fluid in humans examined by pleural lavage. *Am J Respir Crit Care Med* 2000; 162: 1023–1026.
63. Negrini D, Del Fabbro M, Venturoli D. Fluid exchanges across the parietal peritoneal and pleural mesothelia. *J Appl Physiol* 1993; 74: 1779–1784.
64. Negrini D, Venturoli D, Townsley MI, Reed RK. Permeability of parietal pleura to liquid and proteins. *J Appl Physiol* 1994; 76: 627–633.
65. Lai-Fook SJ, Kaplowitz MR. Pleural protein concentration and liquid volume in spontaneously hypertensive rats. *Microvasc Res*: 1987: 101–108.
66. Rossi GA, Sacco O. Cells of the mesothelial space. *In*: Crystal RG, West JB, eds. The Lung: Scientific Foundations. Philadelphia, Lippincott-Raven, 1997; pp. 971–979.
67. Negrini D, Pistolesi M, Miniati M, Bellina CR, Giuntini C, Miserocchi G. Regional protein absorption rate from the pleural cavity in dogs. *J Appl Physiol* 1985; 58: 2062–2067.
68. Negrini D, Ballard ST, Benoit JN. Contribution of lymphatic myogenic activity and respiratory movements to pleural lymph flow. *J Appl Physiol* 1994; 76: 2267–2274.
69. Pappenheimer JR, Renkin EM, Borrero LM. Filtration, diffusion and molecular sieving through peripheral capillary membranes. A contribution to the pore theory of capillary permeability. *Am J Physiol* 1951; 167: 13–46.
70. Michel CC. The transport of albumin: a critique of the vesicular system in transendothelial transport. *Am Rev Respir Dis* 1992; 146: S32–S36.
71. Landis ER, Pappenheimer JR. Exchange of substances through the capillary walls. *In*: Hamilton WF, Down P, eds. Handbook of Physiology, Circulation. Volume 2. Bethesda, American Physiological Society, 1963; pp. 961–1034.
72. Kim K, McIlroy Critz A, Crandall E. Transport of water and solutes across sheep visceral pleura. *Am Rev Respir Dis* 1979; 120: 883–892.
73. Payne DK, Kinasewitz GT, Gonzalez E. Comparative permeability of canine visceral and parietal pleura. *J Appl Physiol* 1988; 65: 2558–2564.
74. Agostoni E, Piper J. Capillary pressure and distribution of vascular resistance in isolated lung. *Am J Physiol* 1962; 202: 1033–1036.
75. Kinasewitz CT, Groome LJ, Marshall RP, Diana JN. Permeability of the canine visceral pleura. *J Appl Physiol* 1983; 55: 121–130.
76. Michel CC. Fluid movements through capillary walls. *In*: Renkin EM, Michel CC, eds. Handbook of Physiology: The Cardiovascular System, Microcirculation. Baltimore, American Physiological Society, 1984; pp. 375–409.
77. Taylor AE, Parker JC. Pulmonary interstitial spaces and lymphatics. *In*: Fishman AP, Fisher AB, eds. Handbook of Physiology: The Respiratory System, Circulation and Nonrespiratory Functions. Baltimore, American Physiological Society, 1985; pp. 167–229.
78. D′Angelo E, Heisler N, Agostoni E. Acid-base balance of pleural liquid in dogs. *Respir Physiol* 1979; 37: 137–149.
79. Song Y, Yang B, Matthay MA, Tonghui MA, Verkman AS. Role of aquaporin water channels in pleural fluid dynamics. *Am J Physiol Cell Physiol* 2000; 279: C1744–C1750.
80. Renkin EM. Transport of large molecules across capillary wall. *Physiologist* 1964; 7: 13–28.
81. Agostoni E, Agostoni PG, Zocchi L. Pleural liquid pressure in the zone of apposition and in the lung zone. *Respir Physiol* 1989; 75: 357–370.
82. Parker JC, Falgout HJ, Grimbert FA, *et al.* The effect of increased vascular pressure on albumin-excluded volume and lymph flow in the dog lung. *Circ Res* 1980; 47: 866–873.
83. Hargens AR, Zweifach BW. Transport between blood and peripheral lymph in intestine. *Microvasc Res* 1976; 11: 89–101.
84. Parker JC, Taylor AE. Comparison of capsular and intra-alveolar fluid pressures in the lung. *J Appl Physiol* 1982; 52: 1444–1452.
85. Miserocchi G, Kelly S, Negrini D. Pleural and extrapleural interstitial liquid pressure measured by cannulas and micropipettes. *J Appl Physiol* 1988; 65: 555–562.
86. Miserocchi G, Negrini D, Gonano C. Direct measurement of interstitial pulmonary pressure in *in situ* lung with intact pleural space. *J Appl Physiol* 1990; 69: 2168–2174.

87. Miniati M, Parker JC, Pistolesi M, *et al.* Reabsorption kinetics of albumin from pleural space of dogs. *Am J Physiol* 1988; 255: H375–H385.
88. Miserocchi G, Negrini D. Contribution of Starling and lymphatic flows to pleural liquid exchanges in anesthetized rabbits. *J Appl Physiol* 1986; 61: 325–330.
89. Agostoni E, Zocchi L. Mechanisms involved in pleural liquid turnover. *J Appl Physiol* 1995; 78: 2329.
90. Berthiaume Y, Staub NC, Matthay MA. Beta-adrenergic agonists increase lung liquid clearance in anesthetized sheep. *J Clin Invest* 1987; 79: 335–343.
91. McHale NG, Roddie IC. The effects of catecholamines on pumping activity in isolated bovine mesenteric lymphatics. *J Physiol* 1983; 338: 527–536.
92. Agostoni E, Zocchi L. Starling forces and lymphatic drainage in pleural liquid and protein exchanges. *Respir Physiol* 1991; 86: 271–281.
93. Negrini D, Del Fabbro M. Subatmospheric pressure in the rabbit pleural lymphatic network. *J Physiol* 1999; 520: 761–769.
94. Broaddus VC, Light RW. General principles and diagnostic approach. *In*: Murray JF, Nadel JA, Mason RJ, Boushey HA Jr, eds. Textbook of Respiratory Medicine. W.B. Saunders, 2000; pp. 1995–2112.
95. Miserocchi G, Negrini D, Mariani E, Passafaro M. Reabsorption of a saline- or plasma-induced hydrothorax. *J Appl Physiol* 1983; 54: 1574–1578.
96. Miserocchi G, Negrini D, Mukenge S, Turconi P, Del Fabbro M. Liquid drainage through the peritoneal diaphragmatic surface. *J Appl Physiol* 1989; 66: 1579–1585.
97. Bodega F, Zocchi L, Agostoni E. Albumin transcytosis in mesothelium. *Am J Physiol Lung Cell Mol Physiol* 2002; 282: L3–L11.
98. Agostoni E, Bodega F, Zocchi L. Albumin transcytosis from the pleural space. *J Appl Physiol* 2002; 93: 1806–1818.
99. Stewart PB, Burgen SV. The turnover of fluid in the dog's pleural cavity. *J Lab Clin Med* 1958; 52: 212–230.
100. Black LF. The pleural space and pleural fluid. *Mayo Clin Proc* 1972; 47: 493–506.
101. Sahn SA. The pleura. *Am Rev Respir Dis* 1988; 138: 184–234.
102. Judson MA, Sahn SA. The pleural space and organ transplantation. *Am J Respir Crit Care Med* 1996; 153: 1153–1165.
103. Kinasewitz GT. Transudative effusions. *Eur Respir J* 1997; 10: 714–718.
104. Light RW, MacGregor MI, Luchsinger PC, *et al.* Pleural effusions: the diagnostic separation of transudates and exudates. *Ann Intern Med* 1972; 77: 505–513.
105. Light RW, Broaddus VC. Pleural effusion. *In*: Murray JF, Nadel JA, Mason RJ, Boushey HA Jr, eds. Textbook of Respiratory Medicine. W.B. Saunders, 2000; pp. 2013–2042.
106. Antony VB, Mohammed KA. Pathophysiology of pleural space infections. *Semin Respir Infect* 1999; 14: 9–17.
107. Light RW. Diagnostic principles in pleural disease. *Eur Respir J* 1997; 10: 476–481.
108. Roth BJ, O'Meara TF, Cragun WH. The serum-effusion albumin gradient in the evaluation of pleural effusion. *Chest* 1990; 98: 546–549.
109. Chakko SC, Caldwell SH, Sforza PP. Treatment of congestive heart failure. Its effect on pleural fluid chemistry. *Chest* 1989; 95: 798–802.
110. Wiener-Kronish JP, Matthay MA, Callen PW, Filly RA, Gamsu G, Staub NC. Relationship of pleural effusions to pulmonary hemodynamics in patients with congestive heart failure. *Am Rev Respir Dis* 1985; 132: 1253–1256.
111. Wiener-Kronish JP, Goldstein R, Matthay RA, *et al.* Chronic pulmonary arterial and right atrial hypertension are not associated with pleural effusion. *Chest* 1987; 92: 967–970.
112. Wiener-Kronish JP, Matthay MA. Pleural effusions associated with hydrostatic and increased permeability pulmonary edema. *Chest* 1988; 93: 852–858.
113. Broaddus VC, Wiener-Kronish JP, Staub NC. Clearance of lung edema into the pleural space of volume-loaded anesthetized sheep. *J Appl Physiol* 1990; 68: 2623–2630.
114. Wiener-Kronish JP, Broaddus VC, Albertine KH, Gropper MA, Matthay MA, Staub NC. Relationship of pleural effusions to increased permeability pulmonary edema in anesthetized sheep. *J Clin Invest* 1988; 82: 1422–1429.
115. Miserocchi G, Negrini D, Del Fabbro M, Venturoli D. Pulmonary interstitial pressure in intact *in situ* lung: the transition to interstitial edema. *J Appl Physiol* 1993; 74: 1171–1177.
116. Eid AA, Keddissi JI, Kinasewitz GT. Hypoalbuminemia as a cause of pleural effusions. *Chest* 1999; 115: 1066–1069.
117. Lieberman FL, Hidemura R, Peters RL, Reynolds TB. Pathogenesis and treatment of hydrothorax complicating cirrhosis with ascites. *Ann Intern Med* 1966; 64: 341–351.
118. Idell S, Girard W, Koenig KB, McLarty J, Fair DS. Abnormalities of pathways of fibrin turnover in the human pleural space. *Am Rev Respir Dis* 1991; 144: 187–194.